Hindawi Publishing Corporation
Journal of Soft Matter
Volume 2013, Article ID 732157, 7 pages
http://dx.doi.org/10.1155/2013/732157

Research Article

An Elastin-Derived Self-Assembling Polypeptide

Antonietta Pepe and Brigida Bochicchio

Department of Science, University of Basilicata, Via Ateneo Lucano, 10, 85100 Potenza, Italy

Correspondence should be addressed to Brigida Bochicchio; brigida.bochicchio@unibas.it

Received 26 April 2013; Accepted 27 May 2013

Academic Editor: Eri Yoshida

Elastin is an extracellular matrix protein responsible for the elastic properties of organs and tissues, the elastic properties being conferred to the protein by the presence of elastic fibers. In the perspective of producing tailor-made biomaterials of potential interest in nanotechnology and biotechnology fields, we report a study on an elastin-derived polypeptide. The choice of the polypeptide sequence encoded by exon 6 of Human Tropoelastin Gene is dictated by the peculiar sequence of the polypeptide. As a matter of fact, analogously to elastin, it is constituted of a hydrophobic region (GLGAFPAVTFPGALVPGG) and of a more hydrophilic region rich of lysine and alanine residues (VADAAAAYKAAKA). The role played by the two different regions in triggering the adoption of beta-turn and beta-sheet conformations is herein discussed and demonstrated to be crucial for the self-aggregation properties of the polypeptide.

1. Introduction

The natural extracellular matrix (ECM) has been, over the years, a source of inspiration for the design and the production of biomaterials of potential interest as scaffolds in tissue engineering [1, 2]. The propensity to self-aggregate, typical of the proteins contained in ECM, into nanostructured fibers and fibrils, makes it strongly attractive. Over the last years, there has been a remarkable progress in the synthesis of ECM protein-inspired polypeptides. Elastin is the ECM protein responsible for the elasticity of organs and tissues such as lungs, skin, and arteries, the elastic properties being conferred on elastin by the presence of fibers [3]. The propensity to self-aggregate was also demonstrated for some soluble elastin derivatives such as α-elastin and κ-elastin and for some short-synthetic peptides [4]. More recently, long elastin-derived polypeptides obtained both by DNA recombinant technologies and by chemical synthesis were investigated and demonstrated to be able to self-aggregate into fibers and fibrils, analogously to the entire protein [5, 6]. In this context, a crucial role is played by the peculiar sequence of the polypeptide [7]. The outstanding mechanical properties of elastin are due to the regular alternance of hydrophobic regions, rich in glycine, alanine, valine, and leucine, and of hydrophilic domains rich in alanine and lysine residues [7]. The hydrophobic sequences give elasticity while the hydrophilic [8] ones confer to the protein resistance to rupture and fatigue. As a matter of fact, the hydrophilic domains are involved in the formation of covalent cross-links occurring between adjacent molecules via the action of lysyl oxidase in the ECM [8]. The polypeptide sequence encoded by exon 6 (EX6) of HTE (GLGAFPAVTFPGALVPGG VADAAAAYKAAKA) can be considered as a "minielastin" with its hydrophobic part (GLGAFPAVTFPGALVPGG) and its alanine-rich crosslinking domain (VADAAAAYKAAKA). In a previous paper, we demonstrated that EX6 is able to self-aggregate into an hydrogel by an irreversible and inverse phase-transition process [9, 10]. Herein, we report the characterization, at molecular and supramolecular level, of EX6 hydrogel. The secondary structure of EX6 hydrogel was assessed in solution by Circular Dichroism (CD) and in solid state by Fourier Transformed Infrared Spectroscopy (FTIR) in KBr and compared with EX6 as a non-aggregated form (lyophilized). The morphology of EX6 as an hydrogel was

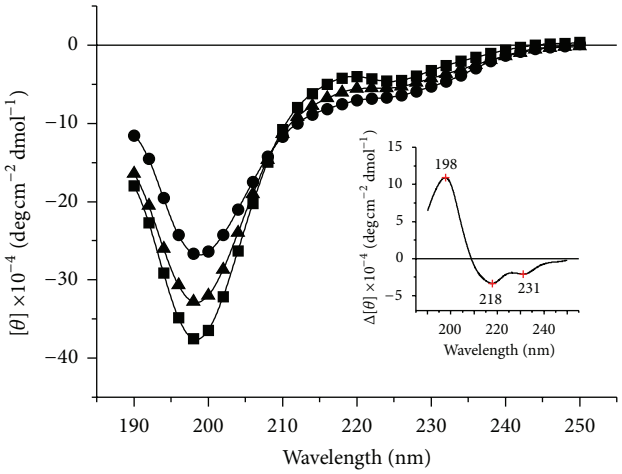

FIGURE 1: CD spectra of EX6 polypeptide recorded in H_2O at different temperatures: 0°C (■); 25°C (▲); 60°C (•). Inset: CD difference spectrum in aqueous solution of EX6 polypeptide. The difference spectrum was obtained by subtracting the curve at 0°C from that at 60°C.

evaluated by Atomic Force Microscopy (AFM). Furthermore, at supramolecular level, EX6 hydrogel was studied by UV and fluorescence spectroscopies.

2. Materials and Methods

The synthesis and purification of EX6 polypeptide were previously described [9].

2.1. CD Spectroscopy. CD spectra of the EX6 lyophilized polypeptide (0.1 mg/mL) were acquired at different temperatures with a Jasco J-815 Spectropolarimeter equipped with a HAAKE thermostat as temperature controller by using 0.1 cm path length quartz cell. Spectra were acquired by taking points every 0.1 nm, with 100 nm/min scan rate, 16 scans, an integration time of 2 s, and a 1 nm bandwidth. The data are expressed in terms of molar ellipticity $[\theta]$, as deg cm^2 dmol^{-1}.

2.2. Thioflavin T (ThT) Fluorescence Assay. The assay for binding of thioflavin T (ThT) was performed according to the method of LeVine [11]. ThT fluorescence emission was measured with excitation at 440 nm between 460 and 500 nm with 5 nm slit widths using a JOBIN YVON-SPEX FLUOROLOG-3 spectrofluorometer. A stock solution of 2.5 mM ThT was prepared in TBS buffer and filtered by a 0.22 μm filter. 1 mL of ThT stock solution was added to 50 mL of TBS to a final concentration of 50 μM. Fluorescence spectra in the presence of EX6 hydrogel were measured. The spectrum of peptide alone was subtracted from the spectrum of the ThT solution with peptide to normalise the fluorescence of the sample by subtracting the blank sample.

2.3. Congo Red Spectral Shift Assay. The procedure described by Klunk et al. [12] was followed, with minor modifications. A Congo red stock solution (1.25 mM) was prepared in TBS buffer/ethanol (8 : 2, v/v) at pH 7.4 and filtered by using a 0.22 μm filter. From this stock solution, a diluted Congo red solution was prepared (0.125 mM). Aliquots (0.350 mL) of EX6 hydrogel were combined with 0.350 mL of the Congo red solution (0.125 mM). The peptide suspensions were stirred, and an absorbance spectrum from 400 to 600 nm was collected with a NIR-UV O5 Cary UV spectrophotometer using quartz cells of 1 cm path length and TBS as reference solution. The spectrum of peptide alone was subtracted from the spectrum of Congo red with peptide to correct for the turbidity of the sample due to the precipitated material.

2.4. FTIR Spectroscopy. The EX6 polypeptide was analyzed by FTIR in KBr pellets (1 mg/100 mg) as a lyophilized powder, as well as EX6 hydrogel. The spectra were recorded on a Jasco FTIR-460 PLUS using a resolution of 2 cm^{-1} and 256 scans and then smoothed by using the Savitzky-Golay algorithm. The decomposition of FTIR spectra was obtained using the peak fitting module implemented in the Origin Software (Microcalc Inc.) using the second derivative method. In the curve fitting procedure, the Voigt peak shape has been used for all peaks. The Voigt shape is a combination of the Gaussian and Lorentzian peak shapes and accounts for the broadening present in the FTIR spectrum.

2.5. Atomic Force Microscopy (AFM). 10 microliters of EX6 hydrogel were deposited on silicon (100) wafer substrate (Aldrich, Saint Louis, MO, USA) and on Mica squares, 0.15 mm thickness, size 15 mm × 15 mm (NT-MDT America Inc., Santa Clara, CA, USA). The silicon wafers were cleaned by using a two-solvent method consisting in the immersion of the Si wafer in warm acetone bath for a period of 10 minutes. Then a methanol bath for a period of 5 minutes immediately followed by final deionized water rinses. The samples were air-dried and repeatedly rinsed with ultrapure water in order to remove salts. After water evaporation, the AFM images were carried out by using the XE-120 microscope (Park Systems) in air and at room temperature. Data acquisition was carried out in intermittent contact mode at scan rates between 0.4 and 3 Hz, using rectangular Si cantilevers (NCHR, Park Systems) having the radius of curvature less than 10 nm and with the nominal resonance frequency and force constant of 330 kHz and 42 N m^{-1}, respectively, or diamond tips (Mikromasch) with typical spike curvature radius less than 7 nm, nominal resonance frequency of 325 kHz, and typical force constant 46 N m^{-1}.

3. Results and Discussion

3.1. CD Spectroscopy. Figure 1 shows the CD spectra in aqueous solution (prefibrillar state) of EX6 as a function of temperature. Furthermore, the conformational study was carried out as a function of the temperature in order to shed light on the conformational transitions of the polypeptide. The CD spectrum in aqueous solution at 0°C is characterized by a strong negative band at 198 nm and by a tendency to adopt a positive theta value at 219 nm (Figure 1(a)). The increase of the temperature to 25 and 60°C induces a

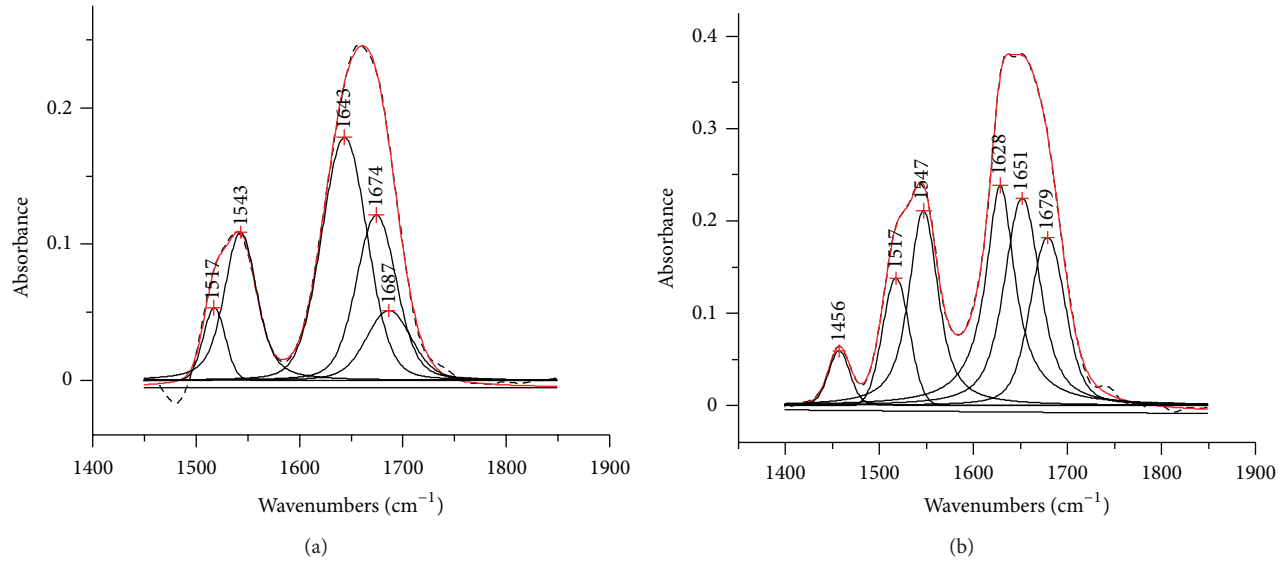

FIGURE 2: Decomposed FT-IR spectra of EX6 polypeptide as lyophilized powder (a) and as fibers (b) in KBr pellets. The band fitting results of Amide I and II regions are shown. Dashed line: experimental spectrum. Solid line: calculated spectrum.

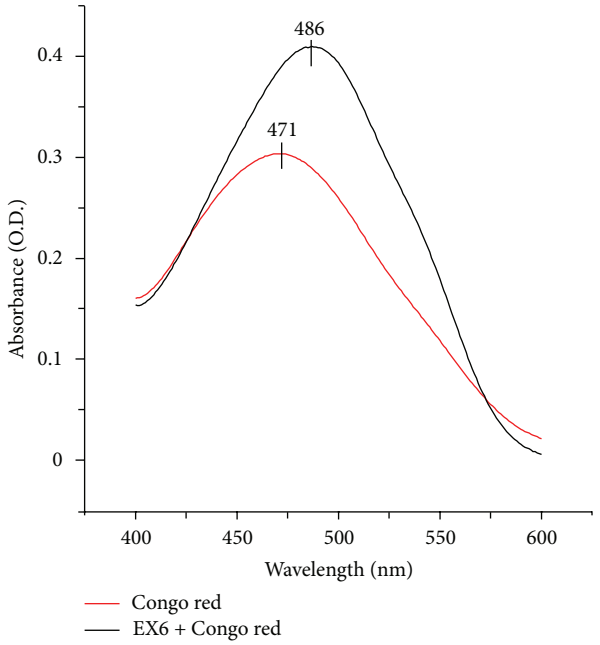

FIGURE 3: Affinity of Congo red to EX6 polypeptide fibers recorded by UV-Vis spectroscopy at room temperature.

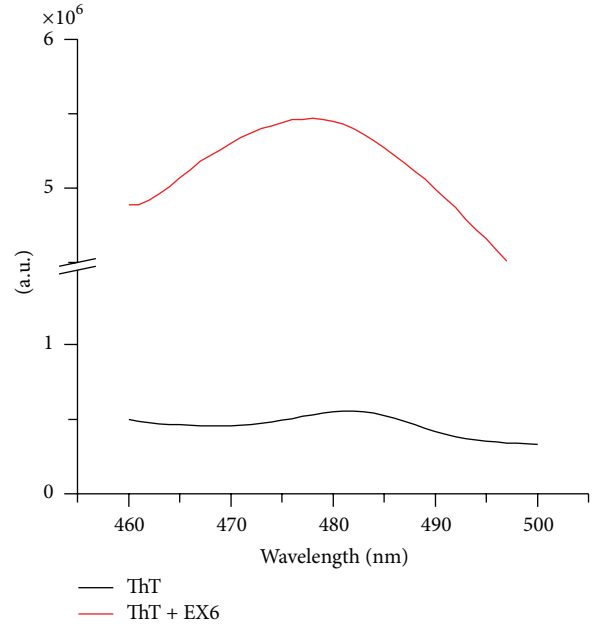

FIGURE 4: Thioflavin T fluorescence graph. Thioflavin T (ThT) 50 μM (black line); EX6 fibers and ThT 50 μM (red line).

progressive reduction of the negative band at 198 nm and the appearance of a weak negative band at 224 nm. These spectral features are indicative of the coexistence of the left-handed polyproline II helix (PPII) and of more unordered conformations [7, 13]. These findings are corroborated by the presence of an isodichroic point at 208 nm indicative of a conformational equilibrium between two different secondary structures [14]. Additional insights into the secondary structure of EX6 polypeptide could be given by the CD difference spectrum obtained by subtracting the spectrum at 0°C from the spectrum at 60°C (inset of Figure 1). The CD spectrum is characterized by a strong positive band at 198 nm and by a weak negative band at 218 nm. These spectral features are indicative of a distorted beta-sheet conformation, stable at high temperatures [15]. Furthermore, a weak negative band at 231 nm could be assigned to unordered conformations [16].

3.2. FTIR in Solid State. Figure 2(a) represents the decomposed FTIR spectrum of Amide I and II regions of EX6 as lyophilized powder. The Amide I region contains a major

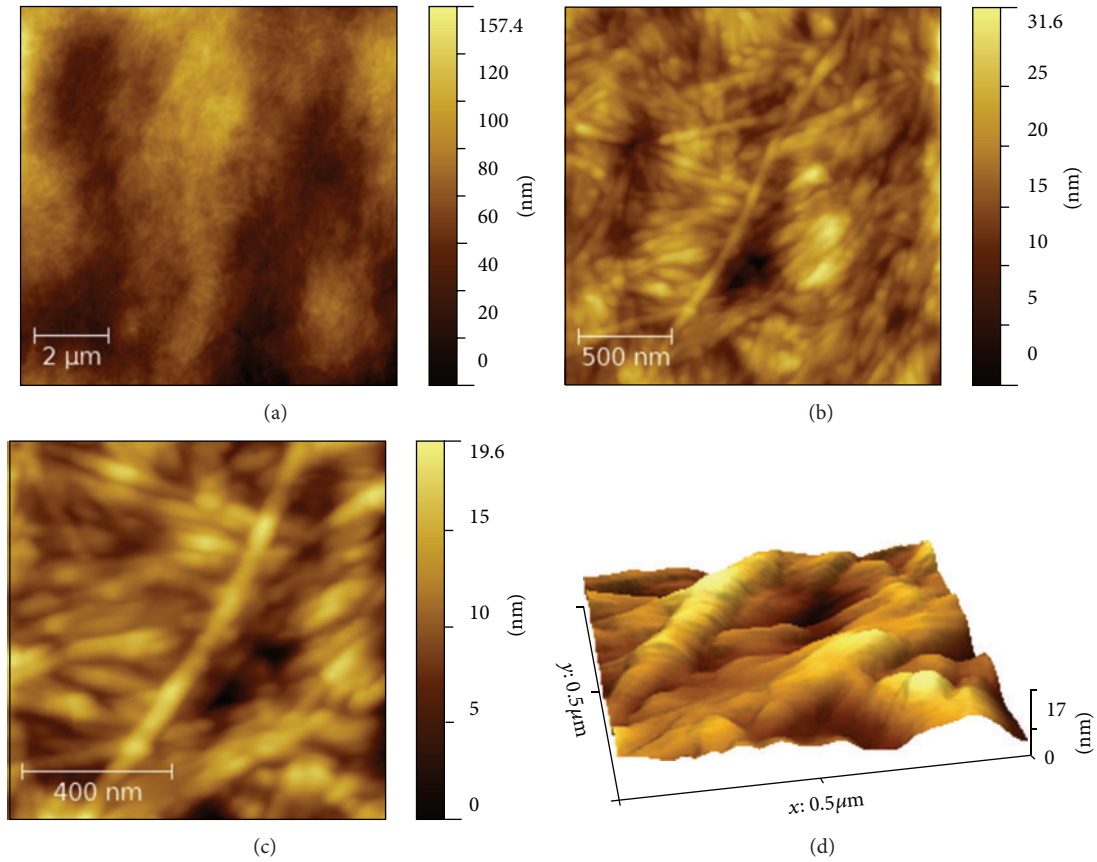

Figure 5: AFM images of EX6 hydrogel deposited on Si(100) substrate observed at different magnification ((a), (b), (c)); 3D rendering of a $0.5 \times 0.5\ \mu$m zone, highlighting the complex texture of the fibers.

component at 1643 cm^{-1} and two minor ones at 1674 and 1687 cm^{-1}. The first component is assigned to water contribution, normally found between 1640 and 1650 cm^{-1} [17]. The component at 1674 cm^{-1} is due to the stretching of non-hydrogen bonded C=O groups compatible with the presence of PPII conformation lacking of intramolecular hydrogen bonds [18]. Finally, the band at 1687 cm^{-1} is indicative of the presence of beta-turns ascribed to the hydrophobic region [19–21]. The Amide II mode of the peptide group is considered a coupled motion involving both N–H bond and C–N bond stretching in the peptide plane and is weaker and less informative than the Amide I. The Amide II region shows two main components at 1543 and 1517 cm^{-1} that could be tentatively assigned to non-hydrogen and hydrogen bonded N–H groups compatible with unordered and beta-turn/beta-sheet conformations, respectively. In Figure 2(b) is shown the decomposed FTIR spectrum of Amide I and II regions of EX6 hydrogel. The main component is centered at [17] 1628 cm^{-1} and is assigned to strongly hydrogen bonded C=O compatible with beta-sheet conformation due to the presence of polyalanine tract. Two minor components are centered at 1651 and at 1679 cm^{-1} and are ascribed to unordered and beta-turn conformation, respectively. We propose for EX6 hydrogel the prevalence of beta-sheet together with unordered conformations present in minor amounts. This interpretation is supported by the observation in the Amide II region of the bands at 1547 and 1517 cm^{-1} assigned to random coil and beta-structures, respectively [20].

3.3. Congo Red Spectral Shift Assay. Congo red is a diazo dye that is widely used to characterize amyloid-like fibers with its binding being specifically dependent on the secondary structure characteristic of the fibrils. It has been demonstrated that the interaction of the Congo red with β-pleated sheet conformation induces two effects in the UV spectrum of peptides, the hyperchromic effect (increase in absorbance) and the bathochromic effect (red shift of maximum absorbance wavelength) [22]. The interaction of EX6 hydrogel with Congo red dye induced both the strong hyperchromic and bathochromic effects (Figure 3).

3.4. Thioflavin-T Fluorescence Assay. Thioflavin-T fluorescence assay represents a useful tool to reveal the presence of amyloid-like fibrils. Thioflavin-T (ThT) is a fluorescent dye suggested to bind rather selectively to the β-sheet structures of amyloid-like fibers [11]. The binding is revealed in the fluorescence spectrum by the increase in the ThT emission band centered at 482 nm [23–25]. The addition of ThT to the EX6 peptide solution induced an increase of the ThT emission band (Figure 4).

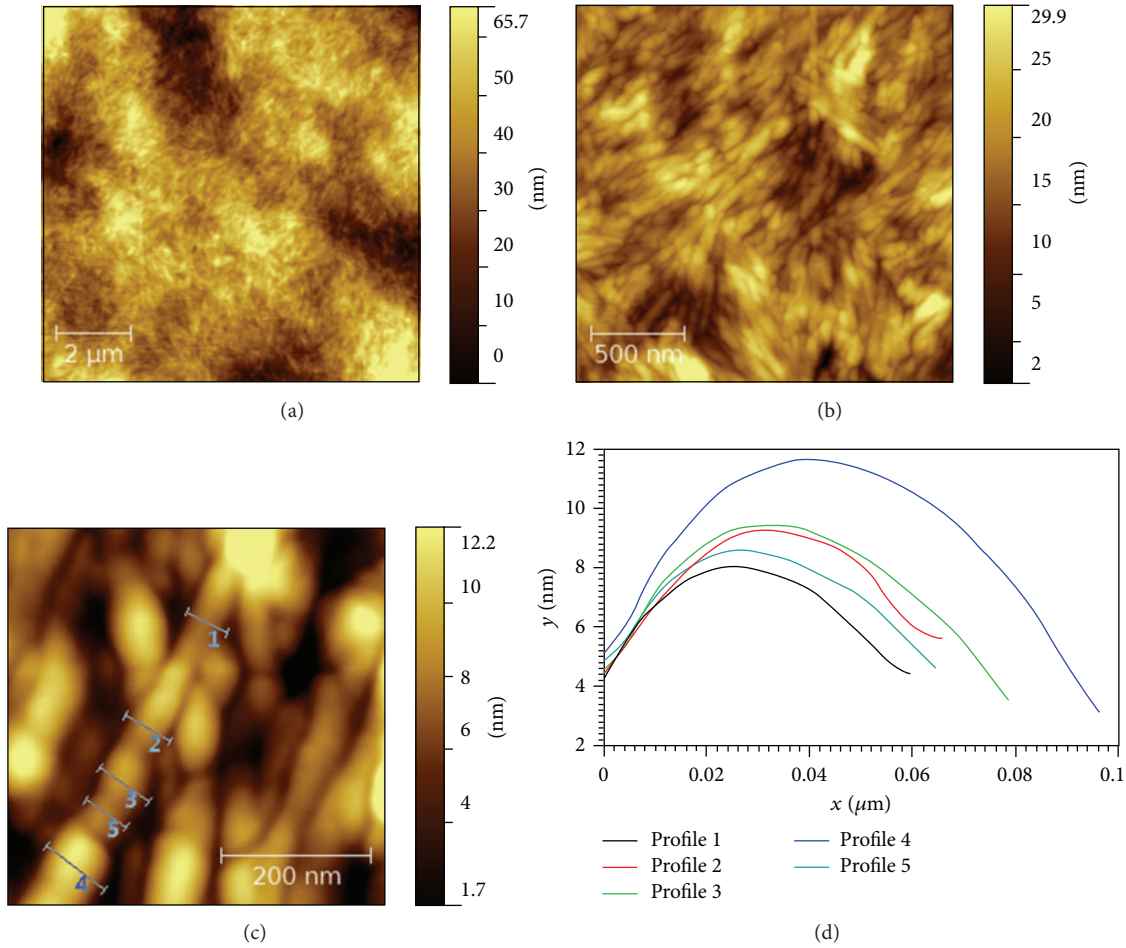

Figure 6: AFM images of EX6 hydrogel deposited on Si(100) substrate observed at different magnification ((a), (b), (c)). In (d) a profile analysis was performed on different position of the fiber visible in Figure (c).

3.5. Atomic Force Microscopy. EX6 hydrogel was deposited onto silicon substrate and investigated by AFM at room temperature and in air. At low magnification a dense network of short and ellipsoidal irregular nanofibers covering completely the substrate is observed (Figure 5(a)). The fibers are side by side aligned. Some longer straight fibers are also discernible (Figures 5(b)–5(c)). At higher magnification the irregularity of the diameter of the fibers was evident (Figures 6(a) and 6(b)). The diameter of the fiber ranges from 60 to 100 nm while the height of the fiber is less than 20 nm, thus suggesting a flattened form of the fibers (Figures 6(c) and 6(d)). While the EX6 polypeptide demonstrated a high tendency to self-assemble in fibrous structures, the morphology observed is different from either beaded necklace structures observed for other elastin polypeptides or highly regular twisted-rope amyloid-like fibers [26]. This observation suggests that the two different regions of the peptide compete during the self-assembly thus producing a peculiar aggregation morphology, with distinctive characteristics.

3.6. Self-Assembly Model. The structural studies carried out in solution and in solid state let us hypothesize a self-assembly mechanism for EX6. The secondary structures found in solution (prefibrillar state) are flexible PPII, favored at low temperature, in equilibrium with beta-sheet conformations. The increase of the temperature shifts the conformational equilibrium from soluble to insoluble beta-sheet structures (inset of Figure 1) responsible for the self-assembly of the polypeptide [27]. As a matter of fact, FTIR studies of EX6 hydrogel show the dominance of beta conformation while only PPII is detectable in EX6 lyophilized powder. The presence of beta-turn as well as of beta-sheet conformation, as revealed by the FTIR results obtained for EX6 hydrogel, could play an important role in the self-aggregation mechanism [28]. Based on the structural studies, a model of self-aggregation for EX6 hydrogel is herein proposed (Figure 7). Both structures are compatible with the primary structure of the polypeptide, as beta-turns are spanning the hydrophobic part of EX6 while beta-sheets concern the poly-alanine tract [29]. On increasing the temperature, extended PPII helices and unordered conformations adopt more folded structures, that is, beta-turn and beta-sheets. Polypeptide chains interact through hydrophobic interactions, giving rise to aggregates. The ellipsoidal aggregates are constituted, at molecular level of beta-turn and unordered conformations quickly interconverting among them.

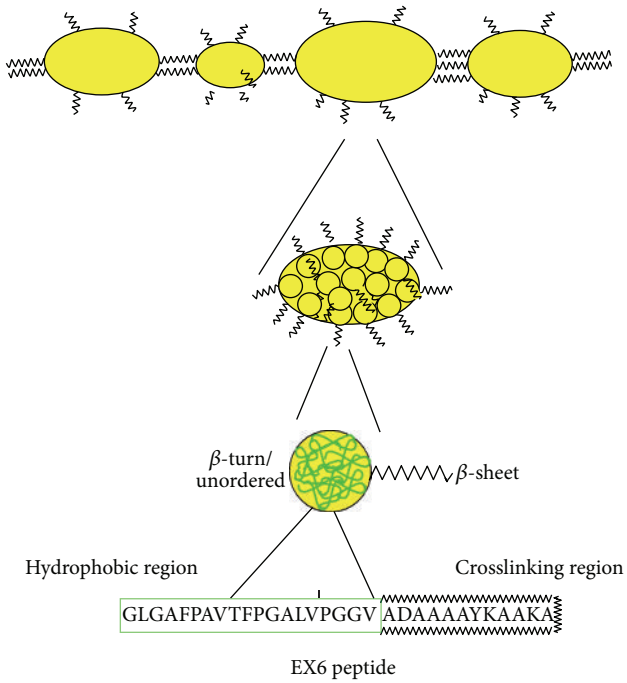

Figure 7: Model for the self-assembly of EX6 into nanofibers.

4. Conclusions

A minielastin represented by EX6 polypeptide is herein reported. The interest of this polypeptide is in its primary structure as composed of a hydrophobic part (GLGAFPAVTFPGALVPGG) and of an alanine-rich crosslinking domain (VADAAAAYKAAKA). The role played by the two different regions in triggering the adoption of beta-turn and beta-sheet conformations is crucial for the self-aggregation properties of the polypeptide [28, 30]. As a matter of fact, the increase of the temperature induces a conformational transition from essentially flexible and unordered conformations to more folded beta-turn and beta-sheet structures responsible for the irreversible precipitation of the soluble polypeptide into insoluble aggregates. The influence of the polypeptide sequence in the adoption of a specific secondary structure is herein demonstrated. This study opens new perspectives in the field of tailor-made elastin-derived peptides and their technological applications in nanotechnology and biotechnology.

Conflict of Interests

The authors certify that no actual or potential conflict of interests in relation to this paper exists.

Acknowledgments

Thanks are due to Dr. Neluta Ibris for AFM images (CIGAS, University of Basilicata) and to Dr. Marina Lorusso for her technical assistance. The financial support from MIUR (PRIN 2010-Project 2010L (SH3K)) is gratefully acknowledged.

References

[1] J. C. Rodriguez-Cabello, L. Martin, A. Girotti, C. Garca-Arévalo, F. J. Arias, and M. Alonso, "Emerging applications of multifunctional elastin-like recombinamers," *Nanomedicine*, vol. 6, no. 1, pp. 111–122, 2011.

[2] D. L. Nettles, A. Chilkoti, and L. A. Setton, "Applications of elastin-like polypeptides in tissue engineering," *Advanced Drug Delivery Reviews*, vol. 62, no. 15, pp. 1479–1485, 2010.

[3] J. E. Wagenseil and R. P. Mecham, "New insights into elastic fiber assembly," *Birth Defects Research C*, vol. 81, no. 4, pp. 229–240, 2007.

[4] A. Pepe, B. Bochicchio, and A. M. Tamburro, "Supramolecular organization of elastin and elastin-related nanostructured biopolymers," *Nanomedicine*, vol. 2, no. 2, pp. 203–218, 2007.

[5] M. Miao, C. M. Bellingham, R. J. Stahl, E. E. Sitarz, C. J. Lane, and F. W. Keeley, "Sequence and structure determinants for the self-aggregation of recombinant polypeptides modeled after human elastin," *Journal of Biological Chemistry*, vol. 278, no. 49, pp. 48553–48562, 2003.

[6] A. Pepe, D. Guerra, B. Bochicchio et al., "Dissection of human tropoelastin: supramolecular organization of polypeptide sequences coded by particular exons," *Matrix Biology*, vol. 24, no. 2, pp. 96–109, 2005.

[7] B. Bochicchio and A. Pepe, "Role of polyproline II conformation in human tropoelastin structure," *Chirality*, vol. 23, no. 9, pp. 694–702, 2011.

[8] J. A. Foster, L. Rubin, and H. M. Kagan, "Isolation and characterization of cross linked peptides from elastin," *Journal of Biological Chemistry*, vol. 249, no. 19, pp. 6191–6196, 1974.

[9] A. M. Tamburro, A. Pepe, and B. Bochicchio, "Localizing α-helices in human tropoelastin: assembly of the elastin 'puzzle'," *Biochemistry*, vol. 45, no. 31, pp. 9518–9530, 2006.

[10] D. Tintar, V. Samouillan, J. Dandurand et al., "Human tropoelastin sequence: dynamics of polypeptide coded by Exon 6 in solution," *Biopolymers*, vol. 91, no. 11, pp. 943–952, 2009.

[11] H. LeVine III, "Quantification of β-sheet amyloid fibril structures with thioflavin T," *Methods in Enzymology*, vol. 309, pp. 274–284, 1999.

[12] W. E. Klunk, R. F. Jacob, and R. P. Mason, "Quantifying amyloid by congo red spectral shift assay," *Methods in Enzymology*, vol. 309, pp. 285–305, 1999.

[13] B. Bochicchio and A. M. Tamburro, "Polyproline II structure in proteins: identification by chiroptical spectroscopies, stability, and functions," *Chirality*, vol. 14, no. 10, pp. 782–792, 2002.

[14] A. F. Drake, G. Siligardi, and W. A. Gibbons, "Reassessment of the electronic circular dichroism criteria for random coil conformations of poly(l-lysine) and the implications for protein folding and denaturation studies," *Biophysical Chemistry*, vol. 31, no. 1-2, pp. 143–146, 1988.

[15] R. W. Woody, "Circular dichroism and conformation of unordered peptides," in *Advances in Biophysical Chemistry*, L. A. Bush, Ed., vol. 2, pp. 37–79, JAI Press, Greenwich, Conn, USA, 1992.

[16] A. Perczel, M. Hollosi, P. Sandor, and G. D. Fasman, "The evaluation of type I and type II β-turn mixtures. Circular dichroism, NMR and molecular dynamics studies," *International Journal of Peptide and Protein Research*, vol. 41, no. 3, pp. 223–236, 1993.

[17] S. Cai and B. R. Singh, "A distinct utility of the amide III infrared band for secondary structure estimation of aqueous protein solutions using partial least squares methods," *Biochemistry*, vol. 43, no. 9, pp. 2541–2549, 2004.

[18] M. Martino, A. Bavoso, V. Guantieri, A. Coviello, and A. M. Tamburro, "On the occurrence of polyproline II structure in elastin," *Journal of Molecular Structure*, vol. 519, no. 1–3, pp. 173–189, 2000.

[19] M. Hollosi, Z. Majer, A. Z. Ronai et al., "CD and Fourier transform ir spectroscopic studies of peptides. II. Detection of β-turns in linear peptides," *Biopolymers*, vol. 34, no. 2, pp. 177–185, 1994.

[20] J. Bandekar, "Amide modes and protein conformation," *Biochimica et Biophysica Acta*, vol. 1120, no. 2, pp. 123–143, 1992.

[21] P. I. Haris and D. Chapman, "The conformational analysis of peptides using Fourier transform IR spectroscopy," *Biopolymers*, vol. 37, no. 4, pp. 251–263, 1995.

[22] W. E. Klunk, R. F. Jacob, and R. P. Mason, "Quantifying amyloid by congo red spectral shift assay," *Methods in Enzymology*, vol. 309, pp. 285–305, 1999.

[23] A. A. Maskevich, V. I. Stsiapura, V. A. Kuzmitsky et al., "Spectral properties of thioflavin T in solvents with different dielectric properties and in a fibril-incorporated form," *Journal of Proteome Research*, vol. 6, no. 4, pp. 1392–1401, 2007.

[24] H. LeVine III, "Stopped-flow kinetics reveal multiple phases of thioflavin T binding to Alzheimer β(140) amyloid fibrils," *Archives of Biochemistry and Biophysics*, vol. 342, no. 2, pp. 306–316, 1997.

[25] H. Naiki, K. Higuchi, M. Hosokawa, and T. Takeda, "Fluorometric determination of amyloid fibrils in vitro using the fluorescent dye, thioflavine T," *Analytical Biochemistry*, vol. 177, no. 2, pp. 244–249, 1989.

[26] A. Pepe, R. Flamia, D. Guerra et al., "Exon 26-coded polypeptide: an isolated hydrophobic domain of human tropoelastin able to self-assemble in vitro," *Matrix Biology*, vol. 27, no. 5, pp. 441–450, 2008.

[27] A. M. Tamburro, A. Pepe, B. Bochicchio, D. Quaglino, and I. P. Ronchetti, "Supramolecular amyloid-like assembly of the polypeptide sequence coded by exon 30 of human tropoelastin," *Journal of Biological Chemistry*, vol. 280, no. 4, pp. 2682–2690, 2005.

[28] D. H. Le, R. Hanamura, D.-H. Pham et al., "Self-assembly of elastin-mimetic double hydrophobic polypeptides," *Biomacromolecules*, vol. 14, no. 4, pp. 1028–1034, 2013.

[29] S. E. Grieshaber, T. Nie, C. Yan et al., "Assembly properties of an alanine-rich, lysine-containing peptide and the formation of peptide/polymer hybrid hydrogels," *Macromolecular Chemistry and Physics*, vol. 212, no. 3, pp. 229–239, 2011.

[30] A. M. Tamburro, M. Lorusso, N. Ibris, A. Pepe, and B. Bochicchio, "Investigating by circular dichroism some amyloidogenic elastin-derived polypeptides," *Chirality*, vol. 22, no. 1, pp. E56–E66, 2010.